3

Imaging of Pheochromocytoma and Paraganglioma

Malak Itani • Joyce Mhlanga

Mallinckrodt Institute of Radiology, Washington University in St. Louis, St Louis, MO, USA

Author for correspondence: Malak Itani, Mallinckrodt Institute of Radiology, Washington University in St. Louis, St Louis, MO, USA. E-mail: mitani9@uw.edu

Doi: http://dx.doi.org/10.15586/paraganglioma.2019.ch3

Abstract: With improvements in genetics and oncology, and increased cross-sectional imaging, there is rapid expansion in the existing knowledge regarding diagnosis and management of pheochromocytomas and paragangliomas (PPGL). According to the 2017 World Health Organization (WHO) Classification of Tumors of Endocrine Organs, genetic cancer susceptibility is more frequent in endocrine cancers, especially PPGL cancers. Imaging plays an important role in the diagnosis and staging of disease, as well as part of surveillance in the heritable syndromes. In this chapter, we review the imaging characteristics of PPGL, under both anatomic and physiologic imaging modalities, supported with multiple clinical examples. We allude to the role of imaging in specific scenarios, such as genetic syndromes, and describe some of the relevant recent advances particularly as related to physiologic imaging.

Keywords: Computed tomography; Magnetic resonance imaging; Positron emission tomography; Single photon emission computed tomography; Somatostatin analogue imaging

In: *Paraganglioma: A Multidisciplinary Approach*. Renato Mariani-Costantini (Editor), Codon Publications, Brisbane, Australia. ISBN: 978-0-9944381-7-1; Doi: http://dx.doi.org/10.15586/paraganglioma.2019

INTRODUCTION

Pheochromocytomas and paragangliomas (PPGLs) present a clinical challenge due to their variable clinical presentation and the high proportion of clinically silent tumors (1), reported to be 76% on an autopsy series published in 1979 (2). With advances in and increased utility of imaging techniques, more cases of silent PPGL are being uncovered. In their review of 201 cases between 1973 and 2007, Kopetschke and colleagues reported that before 1985, less than 10% of cases were discovered incidentally, while this number increased to more than 25% for cases thereafter (3). Recent population studies and advances in the field of genetics have also revealed that PPGLs are associated with underlying germline mutations in up to 41% of cases (4, 5).

Despite increased detection, PPGLs remain relatively uncommon, with an estimated prevalence of 1 in 2000 to 1 in 6500 (4, 6). The importance of radiologic awareness about these tumors lies in their silent presentation and variable radiologic appearance. Typically, paragangliomas of the head and neck arise from parasympathetic ganglia and are non-secretory, while those in the trunk originate from sympathetic ganglia and tend to secrete norepinephrine (7). We will present a radiologic overview of pheochromocytomas and trunk paragangliomas encompassing both morphologic and functional imaging modalities.

IMAGING INDICATIONS

PPGLs can arise in various parts of the body, but they are classified by anatomic location into intra-adrenal and extra-adrenal sites. In contrast to head and neck paragangliomas, abdominal or trunk PPGLs arise from thoracic and abdominal sympathetic ganglia, producing catecholamines (8, 9). Imaging can be utilized at different stages of PPGL disease course. Diagnostic imaging for screening purposes can be offered for patients with germline mutations and high-risk syndromes (Figure 1), such as multiple endocrine neoplasia (MEN) types 2 and 3, von Hippel-Lindau (VHL), neurofibromatosis type 1 (NF1), and succinate dehydrogenase (SDH) mutations (10). This can be done with whole body positron emission tomography (PET) combined with computed tomography (CT) or magnetic resonance imaging (MRI) as in PET/CT or PET/MRI, or with anatomic imaging alone such as MRI or CT of the abdomen and pelvis. The frequency of imaging usually depends on the patient's age and the specific underlying mutation or syndrome.

In patients with clinical suspicion or laboratory evidence of PPGL, imaging is usually performed to localize the lesion and evaluate for any metastatic disease, often with a CT or MRI of the abdomen and pelvis (4). The chest is not usually scanned due to the very low incidence of mediastinal location, estimated at less than 2% of paragangliomas (11). If anatomic imaging is negative, and clinical suspicion is still high, then functional imaging might be the best next step. Genetic testing should be considered for those patients to evaluate for underlying germline mutations or syndromes (4). Early stage surgery is typically curative.

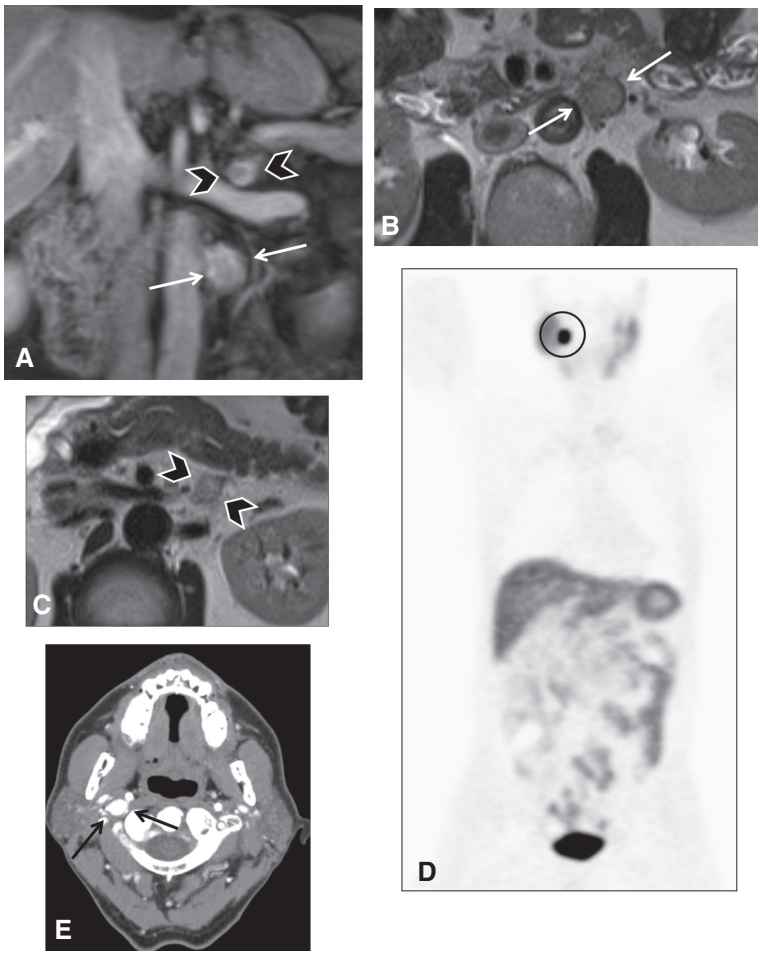

Figure 1 Several neuroendocrine tumors in a 60-year-old male patient with succinate dehydrogenase (SDH) subunit D mutation. (A, B, C) MRI of the abdomen demonstrates two left retroperitoneal lesions, one that is arising from the left adrenal gland (arrowheads) and a larger one more inferiorly, posterior to the fourth segment of the duodenum (white arrows) seen on (A) coronal fat-saturated post-contrast T1-weighted images and (B–C) fast spin echo T2 weighted images. The lesions were surgically resected. The left adrenal lesion was consistent with pheochromocytoma and the more inferior lesions were consistent with paraganglioma. (D) The patient underwent a gallium-68-DOTATATE scan to screen for additional neuroendocrine tumors. This demonstrated intense focal tracer uptake in the right neck (circle). (E) CT angiography and MRI of the neck (not shown) were performed for further characterization and the lesion (black arrow) was consistent with a glomus vagale paraganglioma.

However, patients often present at later stages and once symptomatic. During and after the treatment course, patients will require imaging for restaging and surveillance. Patients with incidentally detected lesions are generally referred for clinical and biochemical evaluation, to be followed by additional imaging if needed.

ANATOMIC IMAGING

The imaging appearance of pheochromocytoma is variable on all imaging modalities and slightly less variable for paragangliomas. This decreases the confidence of radiologic diagnosis for these lesions, although the typical retroperitoneal location and hyper-enhancement assists in narrowing down the differential diagnosis. The classical teaching for PPGLs is the 10% rule, where it was thought that 10% are extra-adrenal, 10% are bilateral, 10% are metastatic, 10% are familial, and 10% are asymptomatic or not associated with hypertension (7). As mentioned earlier, the 10% estimation for familial or genetic predisposition is an underestimate. Moreover, the rate of metastasis for trunk paragangliomas is much higher than that for adrenal pheochromocytomas, reaching up to 60% in some case series (12, 13). As for the location, paragangliomas, also referred to as extra-adrenal pheochromocytomas (EAPs), constitute at least 15% of PPGLs in adults and 30% in children (14). The vast majority of EAPs occur in the retroperitoneal para-aortic region between the diaphragm and the lower poles of the kidneys, with the specific most common location being the organ of Zuckerkandl, between the origin of the inferior mesenteric artery and the aortic bifurcation (7, 15). A small percentage can be in the mediastinum, and in the urinary bladder, with the textbook clinical presentation of the latter being "micturition-induced attack of palpitations and syncope."

Ultrasound

The adrenal glands are easily detected on ultrasound in neonates, but become more challenging to visualize in older children and adults. Adrenal and retroperitoneal lesions may or may not be seen on ultrasound, depending on the lesion size, patient body habitus, and the operator. Ultrasound is not the modality of choice for evaluating or screening for adrenal lesions, pheochromocytomas, or paragangliomas in adults. When detected on ultrasound, pheochromocytomas tend to be of heterogeneous echogenicity and can be partially cystic or necrotic (Figure 2).

Computed tomography

On CT, pheochromocytomas have a higher CT density than adrenal adenomas. A cutoff CT density of less than 10 Hounsfield units (HU) provides 100% sensitivity for diagnosing an adrenal adenoma, with a relatively low specificity of 40.5% (16). This is why, currently, adrenal nodules with a CT density of more than 10 HU undergo further workup. Calcifications have been described in 10–12% of cases of pheochromocytomas and are better appreciated on non-contrast CT (17, 18). Intralesional hemorrhage, cystic changes, and necrosis have also been described with PPGLs, which can give them heterogeneous CT density on noncontrast scans. The imaging appearance of paragangliomas is generally similar to pheochromocytomas (7, 19).

With contrast administration, PPGLs tend to enhance rapidly and avidly due to a rich capillary network (Figures 3 and 4). Adrenal adenomas usually demonstrate milder enhancement than pheochromocytomas or malignant tumors

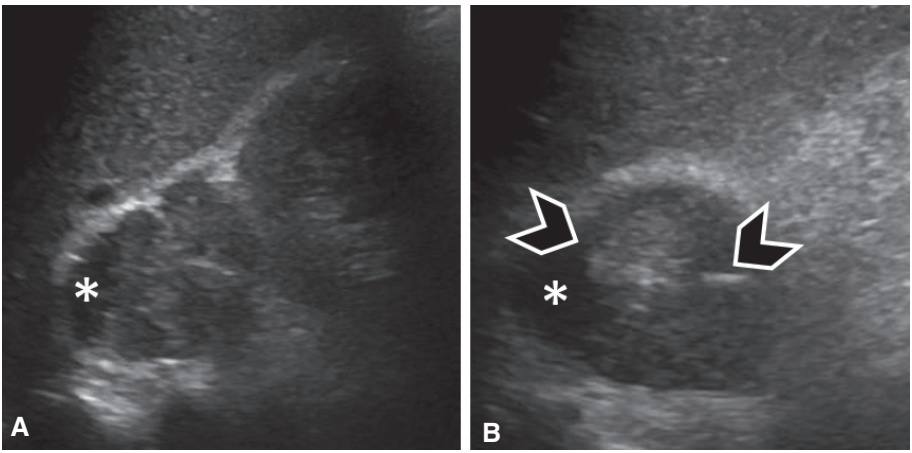

Figure 2 Pheochromocytoma in a 45-year-old male patient. (A) Sagittal and (B) axial ultrasound images of the right adrenal region demonstrate a lesion of heterogeneous echogenicity between the liver (top portion of A and B) and the right kidney (right side of A). The lesion contains a cystic component (asterisk) as well as echogenic foci (arrowheads), suggesting calcifications.

but have faster washout. Absolute washout of more than 60% or relative washout of more than 40% has been previously accepted as being characteristic of benign adrenal adenoma, although more recent studies have suggested that a good proportion of pheochromocytomas, potentially up to one-third, can have washout characteristics similar to benign adenomas (20, 21).

The safety of iodinated contrast administration to patients with pheochromocytomas has been questioned in the past due to incidents of hypertensive crisis after angiography with ionic (high-osmolar) contrast media; there is no evidence, however, of any serious adverse events occurring with the use of newer non-ionic (low-osmolar) iodinated contrast agents and, based on a small prospective study from the National Institute of Health, it is currently considered safe and acceptable to perform contrast-enhanced CT studies for those patients who are not receiving alpha- or beta-blockers (22).

Magnetic resonance imaging

On MRI, like most tumors, pheochromocytomas demonstrate hypointense signal on T1 weighted images and hyperintense signal on T2 weighted images. This rather noncharacteristic appearance renders MR nonspecific for the diagnosis of pheochromocytoma, despite its high sensitivity. Classically, pheochromocytomas were described to have a very hyperintense signal on T2 weighted images, giving them a "light bulb" manifestation; this sign is distinctive in only 10% of lesions but might be helpful in two-thirds[d] of pheochromocytomas (23). Another classical sign of paragangliomas, seen both on T1 and on T2 weighted images, is "salt-and-pepper" appearance, which is seen due to the presence of punctate areas of low-signal intensity corresponding to flow voids from tumor vascularity, and hyperintense signal corresponding to areas of hemorrhage in the tumor. This sign

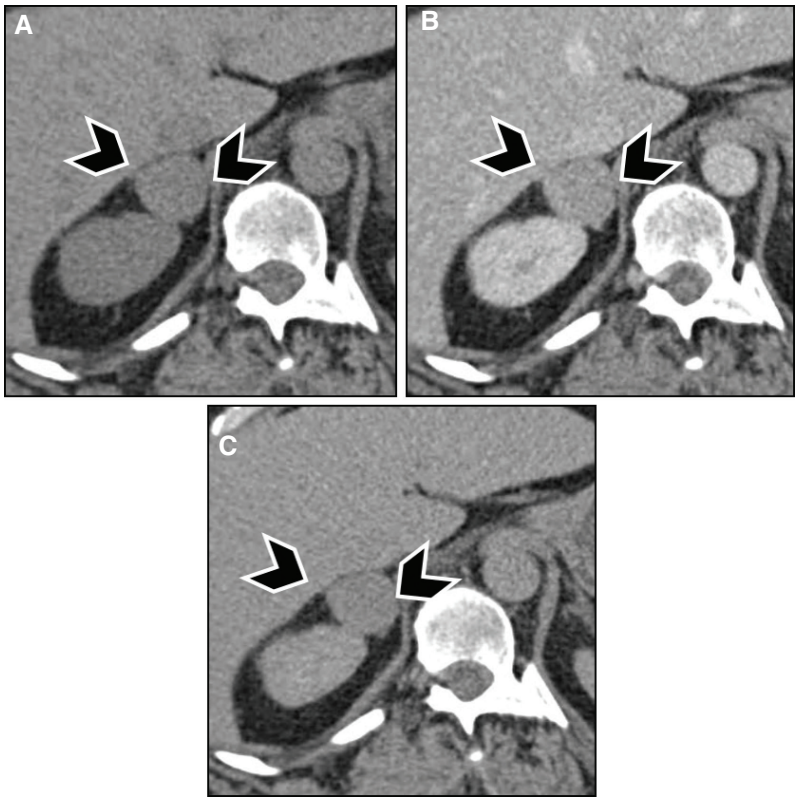

Figure 3 **Pheochromocytoma in a 39-year-old male patient with neurofibromatosis type 1.** (A) Noncontrast images demonstrate a hypodense lesion in the right adrenal gland (arrowheads), with (B) marked enhancement after contrast administration. (C) Adrenal washout phase acquired 15 min after contrast administration demonstrates rapid washout, which is usually seen with adrenal adenomas but can be seen in one-third of pheochromocytomas. The patient had elevated metanephrines, and surgical pathology was consistent with pheochromocytoma.

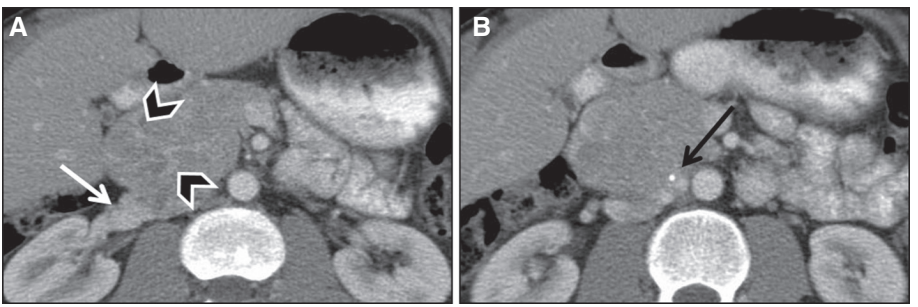

Figure 4 **Paraganglioma in a 30-year-old male patient.** Images obtained after administration of iodinated intravenous contrast demonstrate heterogeneously hyperenhancing retroperitoneal mass compressing the right renal vein (white arrow) with prominent vascular feeders (arrowheads) and a peripheral calcification (black arrow).

has been described more with head and neck paragnagliomas than with trunk paragnagliomas, and is also neither sensitive nor specific, as it can be seen with any hypervascular tumor, namely, in angiofibromas (19). Chemical shift imaging can diagnose intralesional microscopic fat such as that typically seen in adrenal adenomas, but it does not accurately differentiate adenomas from pheochromocytomas because the latter can contain intralesional fat from lipid degeneration (24, 25). Signal heterogeneity within the tumor due to hemorrhage, cystic transformation, and calcifications remains a helpful feature in differentiating pheochromocytomas from benign adenomas (Figure 5). Paragangliomas again demonstrate imaging features similar to pheochromocytomas. Enhancement characteristics on MRI are similar to CT, as PPGLs demonstrate rapid and avid enhancement, but up to one-third of pheochromocytomas have overlapping washout characteristics with adrenal adenomas (20, 21).

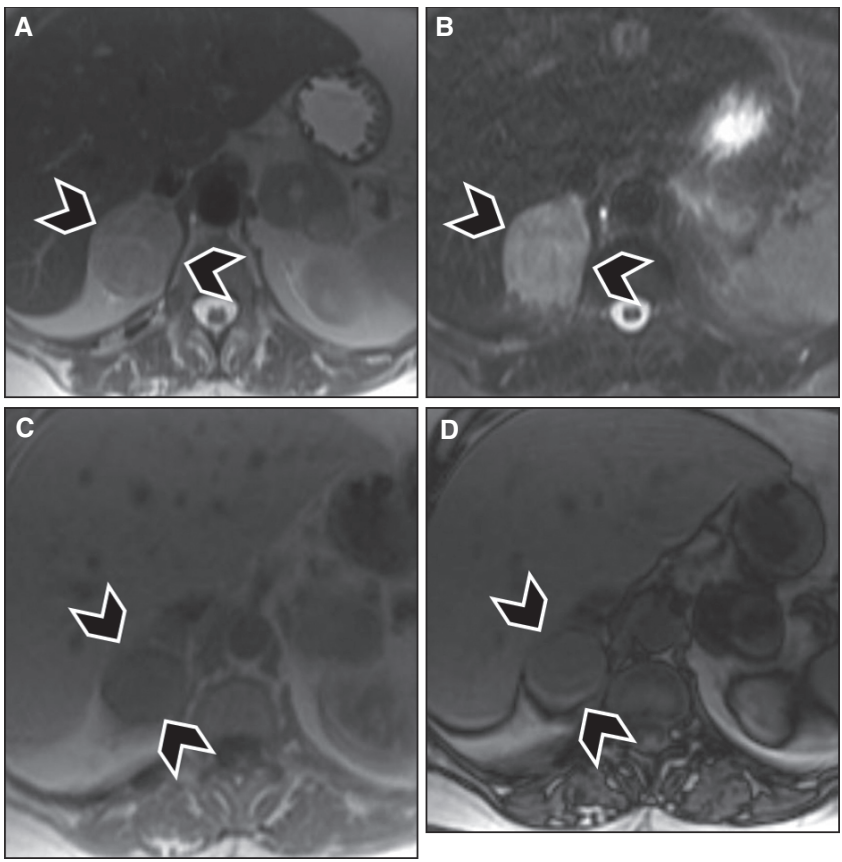

Figure 5 Right adrenal pheochromocytoma (arrowheads) in a 72-year-old female patient. Nonspecific signal intensity characteristics are seen, with intermediate to hyperintense signal seen on (A) T2-weighted images and (B) fat-suppressed T2-weighted images (turbo Inversion Recovery sequence), and hypointense signal seen on (C) in-phase T1-weighted images, and no signal loss on (D) out-of-phase images to suggest intralesional microscopic fat.

PHYSIOLOGIC IMAGING

An advantage of functional imaging or scintigraphy over anatomic imaging is imaging the physiologic basis of disease, as well as the ability to perform whole body imaging, which is useful in the localization of extra-adrenal tumors, metastases, and evaluation of recurrent disease. Functional imaging helps to maximize sensitivity and specificity for the detection of PPGLs, which often have a variable presentation, with nonspecific anatomic imaging appearance. Diagnosis can be challenging due to their heterogeneous location and inconsistent presentation.

Nuclear scintigraphy

With scintigraphy, whole body planar two-dimensional images can be performed followed by dedicated single photon emission computed tomography (SPECT), which can be fused or co-registered with CT images (SPECT/CT) of a specified body region to improve localization and detection of lesions which might be obscured by normal background activity, for example, the liver, bowel, or kidneys. SPECT/CT allows direct simultaneous correlation of functional and anatomic imaging. Whole body scintigraphy has the advantage of demonstrating additional sites of disease, which is especially useful in several of the syndromes associated with PPGLs, and could be used for screening, followed by dedicated anatomic imaging. Functional imaging examinations are performed using I-131 and I-123 metaiodobenzylguanidine (MIBG), In-111 pentetreotide (Octreoscan, Covidien), and several PET ligands including F-18 fluorodopamine, 18F-dihydroxyphenylalanine (DOPA), F-18 fluoro-2-deoxy-D-glucose (FDG), and Ga-68 [DOTA-0-Tyr-3] octreotate (DOTATATE) (10). Ga-68 DOTATATE is a PET radiopharmaceutical linked to a peptide that binds to somatostatin receptors (SSTRs), and it represents the first approved PET agent for somatostatin receptor imaging in the United States by the Food and Drug Administration (FDA), and the only one so far.

Iodine-123 (I-123) or iodine-131 (I-131) meta-iodobenzylguanidine scintigraphy

MIBG is the most common and available imaging technique in the functional assessment of pheochromocytomas and has historically been the gold standard. MIBG is a structural and functional analog of norepinephrine and guanethidine. Uptake occurs chiefly via the energy-dependent type I amine uptake mechanism with initial localization to presynaptic adrenergic nerves in the adrenal medulla, sympathomedullary tissue, and neural crest tumors derived from chromaffin tissue. Retention of MIBG within the cytoplasmic intravesicular neurosecretory granules permits scintigraphic detection in the adrenal medulla, pheochromocytomas, extra-adrenal paragangliomas, and neuroblastomas.

The uptake of radiotracer is proportional to the neurosecretory granule density within the tumor (26, 27). PPGL typically appears as intense focal MIBG uptake, with high tumor-to-background ratio (28, 29). The sensitivity of I-123 MIBG has been reported to range from 77 to 95%, with a specificity of 95–100% (26, 30–33).

Scenarios where MIBG has lower sensitivity for PPGL include tumors above the diaphragm (34, 35), small tumors, or those that are necrotic and/or dopamine secreting (36, 37), and sometimes metastatic disease (38). The lower sensitivity has also been attributed to the variable affinity of MIBG to the amine transport system, the variable amount of cytoplasmic storage granules, and the loss of the amine transport system in dedifferentiated tumors (10, 26). MIBG has a reported false negative rate of 13% mainly due to the lack of sufficient tracer uptake in the lesion for reasons discussed above (39, 40).

SPECT/CT improves sensitivity and specificity (Figure 6); in one case series, MIBG SPECT/CT was shown to increase diagnostic certainty in 89% of discordant CT and planar MIBG cases (41, 42).

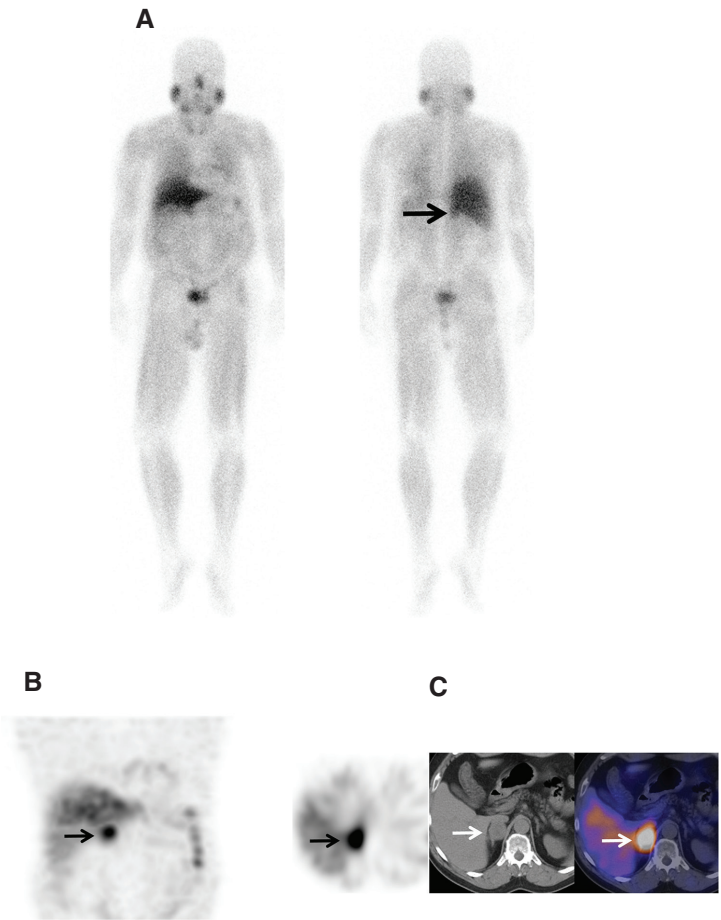

Figure 6 A 40-year-old male patient with elevated catecholamines. (A) Whole body planar images, (B) coronal and axial attenuation-corrected SPECT images, and (C) axial non-enhanced CT and fused SPECT/CT images of the right adrenal region demonstrate a 4 cm × 3 cm × 4 cm soft tissue lesion with intense I-123 MIBG uptake much greater than hepatic uptake consistent with a biopsy-proven pheochromocytoma.

MIBG can be labeled with either I-131 or I-123. Although it is more expensive, I-123 MIBG is the preferred radiopharmaceutical because it produces much better image quality with lower radiation exposure, particularly in children, and has now largely replaced imaging with I-131 MIBG. MIBG is cleared primarily by the kidneys and is not dialyzable; it should not be used in anephric patients. The use of this radiopharmaceutical should be avoided in pregnant and breast-feeding patients. Radiation dose to the thyroid gland should be minimized by blocking of thyroidal radioiodine uptake or free iodide, with stable iodine administered orally, typically with a saturated solution of potassium iodide (29). Many drugs interfere with uptake of MIBG, particularly tricyclic antidepressants, sympathomimetics (e.g., pseudoephedrine), and certain anti-hypertensives (e.g., labetalol, reserpine, and calcium channel blockers) (43). Several mechanisms of pharmacological interaction have been described, including inhibition of the sodium-dependent uptake system and of active transport into storage vesicles, competition for transport into vesicles, depleted storage vesicle content, and calcium mediation, among others.

Somatostatin receptor scintigraphy/somatostatin analogue imaging

SSTRs are expressed in many cells and majority of tumors of neuroendocrine origin including PPGLs (44), which can express SSTRs, which allows the use of somatostatin receptor imaging in the diagnostic process. Somatostatin is a naturally produced 14 amino acid peptide. Five SSTRs have been characterized to date, including SSTR1, 2 (A and B), 3, 4, and 5, with SSTR-2 and SSTR-5 expressions exhibited in 70–90% of all NETs (45, 46). Somatostatin hormone itself is not useful for therapy or imaging, with a short biologic half-life of 2–4 min. Several radiopharmaceuticals have been developed that bind to somatostatin receptors and can be used to image PPGLs, with less rapid enzymatic degradation and a longer half-life of 1.5 to 2 h (44).

Indium (In)-111

In-111 pentetreotide (Octreoscan) is produced by chelating the radionuclide In-111 to octreotide (an 8 amino acid somatostatin analogue) by diethylenetriamine penta-acetic acid (DTPA). In-111 is produced in a cyclotron and decays by electron capture and has a physical half-life of 67 h. It emits principal gammas at 174 and 247 kiloelectron volts (keV). It detects neuroendocrine tumors that contain SSTRs, including vasoactive intestinal peptide tumors, insulinomas, gastrinomas, and PPGLs. In-111 pentetreotide is a conjugate of octreotide that binds to SSTRs on a variety of cells. This octapeptide concentrates in tumors containing a high density of SSTRs for example, neuroendocrine and some non-neuroendocrine tumors. In addition to these tumors, normal organs such as the pituitary, thyroid, spleen, liver, kidneys, and urinary bladder are also visualized, and this agent is taken up in some granulomatous and autoimmune processes due to the presence of SSTR-positive activated mononuclear leukocytes.

Due to its long half-life, whole body In-111 planar images are typically performed after 24 h and once interfering background activity is renally cleared, followed by SPECT/CT that increases the sensitivity to detect SSR-positive disease and provides better anatomic and functional lesion delineation versus planar imaging alone (47). Imaging after 48 h may be performed if there is persistent

bowel activity, which may mask disease in the abdomen. The radiopharmaceutical is rapidly cleared predominantly by the kidneys, with >90% clearance by 24 h. There is early uptake in the lungs, spleen, and blood pool. At 24 h, splenic uptake is greater than liver and bone marrow, as well as the kidneys. There is less uptake in the gallbladder, bowel, bladder, thyroid, and pituitary gland. There is some hepatobiliary clearance into the bowel, and laxatives can be used to clear bowel activity to aid in the interpretation of abdominal images.

Some normal tissue can also express SSTRs, leading to visualization of SSTR-positive "lesions" that are not related to pathology, often termed false-positive findings (48). Examples include the visualization of the gallbladder, thyroid abnormalities, accessory spleens, recent cerebrovascular accidents, and activity at the site of a recent surgical incision (48, 49). A 4-point scale, termed the Krenning scale, for visual grading of scintigraphic uptake using In-111 pentetreotide was developed based on the ratio of tumor:liver uptake(49). Sensitivity for detection of pheochromocytomas and neuroblastomas with SSTR imaging is comparable to that of MIBG scintigraphy, although SSTR imaging has a higher sensitivity for detection of nearly all other neuroendocrine tumors than MIBG scintigraphy.

In-111 pentetreotide is not typically considered a first-line diagnostic tool for imaging metastatic pheochromocytomas and it is also taken up by granulomas, autoimmune diseases and other tumors which could be potential causes of false-positives (50, 51). It is mainly used for the assessment of dedifferentiated pheochromocytomas that no longer express the amine transporter system (MIBG-negative), detection of metastases (10, 50), and detection and staging of other neuroendocrine tumors containing SSRs, especially carcinoid tumors, paragangliomas (Figure 7), gastrinomas, and other pancreatic islet cell tumors. Most paragangliomas are readily detected by In-111 scintigraphy, which often detects additional lesions or other metastatic foci. There are some limitations to SSTR scintigraphy with In-111 pentetreotide, including reduced detection of smaller lesions compared to DOTATATE PET imaging, and high physiologic background uptake, for example, in the liver, because of the suboptimal physical characteristics of the radiopharmaceuticals and the lower resolution of gamma cameras (52).

POSITRON EMISSION TOMOGRAPHY

Several PET radiopharmaceuticals are in production and readily available for use in the diagnostic workup of PPGLs. PETCT provides higher resolution images, with greater signal-to-noise ratio relative to SPECT/CT. The newer time-of-flight imaging also results in greater sensitivity.

F-18 Fluorodeoxyglucose PET/CT

^{18}F-FDG is a glucose analog that becomes trapped within cells and is not dephosphorylated. Uptake reflects metabolism, usually increased in tumors. The role of FDG PET in PPGL is usually secondary, for evaluating dedifferentiated tumors that may be heterogeneous on SSTR imaging with In-111 or Ga-68 DOTATATE, and can exhibit a flip-flop phenomenon in tumors that lack SSRs or an amine

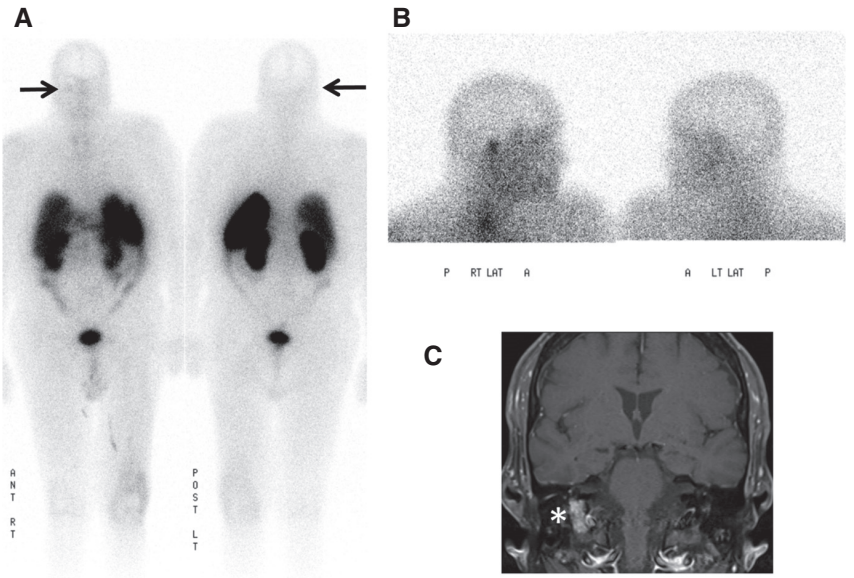

Figure 7 A 65-year-old male patient with right middle ear cavity mass. (A) In-111 pentetreotide whole body planar and (B) lateral spot images of the head performed 24 h after administration of radiotracer show moderate focal tracer uptake in the region of the right middle ear. (C) T1-weighted fat-suppressed post-contrast coronal brain MRI shows an avidly enhancing mass in the right jugular foramen concerning for a glomus tumor. Surgical pathology showed a 1.2 cm × 0.6 cm × 0.3 cm lesion with positivity for synaptophysin and chromogranin on immunohistochemistry, compatible with a paraganglioma.

transport system (53). FDG PET is a useful modality for detecting and confirming metastases in patients with a primary extra-adrenal tumor that is FDG PET-positive (10). FDG PET has been proposed for the localization of neoroendocrine tumors (NETs) and high-grade poorly differentiated NETs with aggressive behavior and for the prognosis and localization of synchronous/metachronous non-NET malignancy. Increased FDG uptake is also seen with mutations involving one of the genes encoding the SDH complex, while lower uptake can rule this out (53). It has also been noted that head and neck paragangliomas arising in the parasympathetic chain may show very low uptake, unlike tumors arising from the sympathetic nervous system (53).

Gallium-68 PET/CT SSTR analogues

SSTR PET uses somatostatin analogs (SSAs) with 68Ga-1,4,7,10-tetraazacyclododecane-1,4,7,10-tetraacetic acid (DOTA)-conjugated peptides for imaging. These could include agonists such as Ga-68 [DOTA-0-Tyr-3] octreotide (DOTATOC), DOTATATE and 68Ga-DOTA,1-Nal3-octreotide (68Ga-DOTANOC), or antagonists such as 68Ga-NODAGA-JR11 (68Ga-OPS202) (54). These PET agents have emerged in the last decade as very strong and accurate imaging tools. Gallium-68 SSTR analogues all have high affinity binding to SSTR subtypes 2 and 5 (55). These are radiolabeled SSTR analogues, similar to In-111

pentetreotide, but coupled with a positron emitter and hence enable imaging by PET/CT or PETMR, offering higher resolution and better imaging characteristics compared to planar or SPECT imaging with In-111 pentetreotide.

Gallium 68 is a positron emitter produced from a Germanium generator. Ge 68 has a T ½ of 270.8 days, and the generator can be used for 6–12 months. Ga-68 has a T ½ of 68 min. There are currently three available Ga-68 DOTA conjugate peptides for PET imaging, including 68Ga-DOTATOC, 68Ga-DOTANOC, and 68Ga-DOTATATE (56). Affinity for SSTRs varies, and DOTA-NOC has added affinity for SSTR3 (57).

Ga-68 DOTATATE, with affinity to SSTR 2 and 5, was approved for use by the FDA in June 2016 (NETSPOT®).[68] Ga-DOTATATE is indicated for localization of SSTR-positive NETs in both adults and children. Typical normal biodistribution is uptake in the pituitary, thyroid, adrenals, liver, spleen, uncinate process of pancreas, kidneys, and bladder. The method of evaluation is similar to octreoscan. Focal increased activity, not typical of normal distribution, is suspicious for disease (Figures 8 and 9). Similar to In-111 pentetreotide, false-positive findings can be seen and misinterpreted, and it is important to be aware of normal distribution and variants. No set diagnostic criteria currently exist for DOTATATE imaging, although there has been a proposal to standardize the reporting criteria using a 5-point structured system (54).

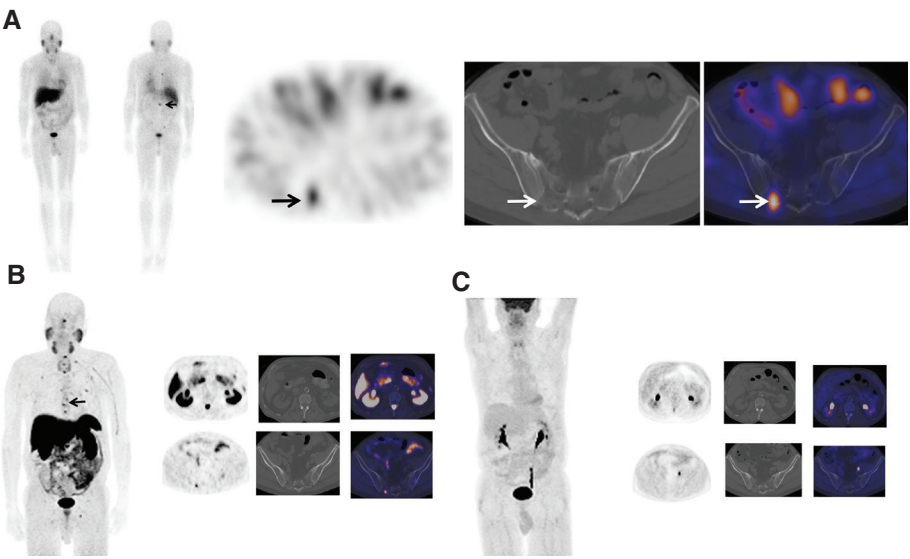

Figure 8 A 60-year-old woman with familial paraganglioma/pheochromocytoma syndrome status after right adrenalectomy with increased plasma metanephrine levels. (A) Previous whole body planar I-123 MIBG scan with attenuation-corrected SPECT, CT, and fused SPECT/CT images show increased uptake in multiple osseous lesions (white arrows). The patient was subsequently treated with I-131 MIBG therapy. (B) Ga-68 DOTATATE PET/CT maximum intensity projection (MIP) image of the skull vertex to the proximal thigh performed 5 years post-therapy because of increasing tumor markers shows widespread somatostatin receptor-positive bone metastatic disease with marked tracer uptake (arrows). (C) An F18-FDG PET/CT performed 1 week prior showed minimal to no uptake in corresponding osseous lesions.

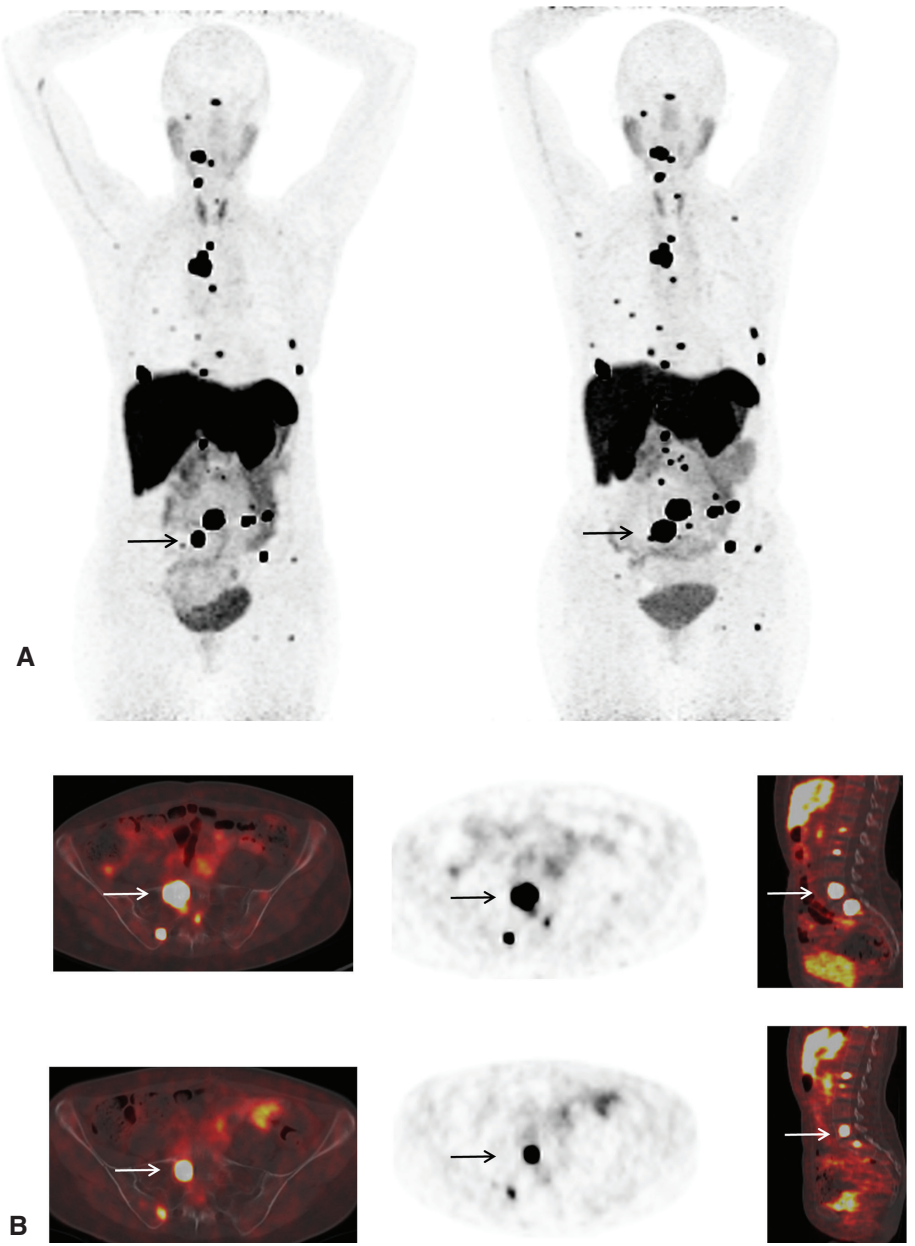

Figure 9 A 55-year-old woman with metastatic paraganglioma having an initial Ki67 proliferation index of 25% and strong SSTR2A immunostain but without SDHB mutation on germline testing. (A) Ga-68 DOTATATE PET/CT maximum intensity projection (MIP) images of the skull vertex to the proximal thigh on the left show widespread somatostatin receptor-positive metastatic disease, with progressive disease on the right image with enlarging pelvic osseous lesions (arrows). (B) Ga-68 DOTATATE PET/CT axial fused PET/CT, axial PET, and sagittal fused PET/CT images show enlarging vertebral lesion (arrows) on the current study (top images) as compared to the prior (bottom images).

A clinical question or scenario that often arises is whether Ga-68 DOTATATE imaging should be performed while patients are on SSAs. Patients on long-acting SSAs usually receive their treatment every 4 weeks, and the routine practice is to schedule the study directly before the next scheduled dose, which permits a time period of at least 3 weeks after the long-acting SSA. SSTR imaging after recent long-acting SSA therapy administration might alter the biodistribution in a way that makes the tumor more conspicuous, leading to an apparent "pseudoprogression," as it results in increased intensity of tracer uptake within metastases, with decreased background uptake in the thyroid, spleen, and liver (58). The authors suggested that pre-dosing with SSA prior to peptide receptor radionuclide therapy (PRRT) may enable higher doses to be delivered to tumor while decreasing dose to normal tissues. Kwekkeboom (49) described this before in relation to SSA therapy prior to scintigraphy with In-11 pentetreotide, describing the possibility of diminished uptake in the spleen due to ongoing treatment with (unlabeled) octreotide, which may be accompanied by a lower liver uptake. This could be misinterpreted as "increased" uptake in the case of liver metastases. However, neuroendocrine tumors often remain visible during treatment with unlabeled octreotide as not all the SSTRs are occupied by the cold/unlabeled octreotide despite high-dose therapy. Thus, in practice, based on available evidence so far, it is acceptable to perform Ga-68 DOTATATE study regardless of the timing related to SSA therapy.

18F-fluorodopamine and 18F-fluorodopa PET/CT

18F-fluorodopamine and 18F-DOPA (6-fluoro dopamine-3,4-dihydroxy-phenylalanine) PET/CT have been used to image noradrenaline and amino acid transporter expression, respectively. 18F-DOPA, a precursor to dopamine, is a well-established tool to explore pheochromocytomas (28).

18F-DOPA is thought to be a better substrate for the amine transport system than norepinephrine and DOPA and may yield improved sensitivity over MIBG in metastatic pheochromocytomas, MEN2-related tumors, SDH iron-sulfur subunit-negative tumors, and SDH-positive lesions (59). There is reported higher accuracy of 18F-DOPA for imaging well-differentiated neuroendocrine neoplasms as compared to conventional imaging and gamma camera scintigraphy, with the main clinical indication being tumors with low/variable SSTR expression (57). It has been noted that PPGLs associated with the parasympathetic system typically demonstrate intense uptake with 18F-fluorodopamine,18F-FDOPA, or 68Ga-labelled DOTA-coupled peptides, regardless of their genetic profile (57).

Fluorine-18-fluorodopamine has a reported sensitivity of up to 100% for primary pheochromocytomas and has depicted pheochromocytomas that were occult on MIBG imaging (26). 18F-DOPA also has limited availability and synthesis is costly; these factors limited its widespread use.

RECENT ADVANCES IN IMAGING

Recent advances in the fields of imaging and nuclear medicine correlate mostly to the introduction of new targeted imaging agents, such as PET imaging of SSTRs, as well as targeted therapeutic agents.

18F-meta-fluorobenzylguanidine

18F-MFBG appears highly promising for imaging of patients with NETs, especially children, allowing for same-day imaging (60). This has advantages over I-123 MIBG scintigraphy, with the use of a PET imaging agent that would allow for same-day imaging with superior resolution and quantitation of the tracer uptake in lesions associated with PET imaging compared to planar or SPECT scintigraphy, and without the need of thyroid blockade.

Treatment and treatment response evaluation

Radionuclide therapy involves systemic administration of targeted radiolabeled peptides with high affinity to the relevant receptor. Treatment with 131I-MIBG has been successfully used in malignant and metastatic pheochromocytomas as an adjunct to surgery and chemotherapy (61, 62). Lutetium 177 DOTATATE therapy has also been used in metastatic PPGLs.

I-131 MIBG therapy

The specific high uptake of MIBG in neuroectodermal tumors, including PPGLs, has led to the development of high-dose I-131 MIBG as a semi-selective therapeutic agent to treat metastatic PPGLs in refractory cases who failed conventional therapy, or as an adjunct to conventional therapies. Several series have demonstrated a moderate objective response rate, symptomatic relief, and some improvement in overall survival (61). A disadvantage of this therapy is that it is ineffective in tumors that do not take up MIBG. There are also possible side effects associated with the administration of therapeutic high-dose, which can cause myelosuppression, but is usually well tolerated, with objective responses observed with high doses (61).

Peptide receptor radionuclide therapy

For treatment of tumors that do not take up MIBG, alternatives exist with the use of PRRT using SSR analogues. These have historically included high-dose octreoscan, with the more recent introduction of lutetium 177-DOTATATE and yttrium-90 DOTATATE therapy, with receptor-mediated internalization of the radiopeptide that can deliver high doses of radiation to the tumor (63–68). Lutetium 177 DOTATATE has been available in Europe since the 1980s and was approved in the United States more recently. Lutetium 177 has 2 gamma peaks at 113 and 208 keV, respectively, which makes it suitable for imaging with a gamma camera for post-therapeutic dosimetry. Yttrium-90 has a half-life of 2.7 days, whereas the physical half-life of lutetium 177 is about 6.7 days.

CONCLUSION

PPGLs often present a challenging clinical diagnosis due to nonspecific symptoms or lack of symptoms. Increased cross-sectional imaging has led to an apparent increase in the incidence of PPGLs, while advances in genetics have led to

improved understanding of PPGLs and indicated a high incidence of associated genetic syndromes. Anatomic imaging provides a readily available tool for screening of these lesions, but lacks specificity due to their variable imaging appearance. Functional imaging provides several options for evaluating PPGLs as they constitute a rare form of neuroendocrine tumors, including but not limited to MIBG and pentetreotide as planar imaging and SPECT agents, and Ga-68 DOTATATE as a PET agent. Nuclear medicine also provides targeted molecular therapy with MIBG, and somatostatin-targeted radioactive lutetium or yttrium.

Conflict of interest: The authors declare no conflicts of interest with respect to research, authorship, and/or publication of this book chapter.

Copyright and permission statement: To the best of our knowledge, the materials included in this chapter do not violate copyright laws. All original sources have been appropriately acknowledged and/or referenced.

REFERENCES

1. Lloyd R, Osamura R, Klöppel G, Rosai J. WHO classification of tumours of endocrine organs. 4th ed. 2017. Lyon: International Agency for Research on Cancer.
2. Sutton MG, Sheps SG, Lie JT. Prevalence of clinically unsuspected pheochromocytoma. Review of a 50-year autopsy series. Mayo Clin Proc. 1981;56(6):354–60. http://dx.doi.org/10.1016/S0022-5347(17)53807-0
3. Kopetschke R, Slisko M, Kilisli A, Tuschy U, Wallaschofski H, Fassnacht M, et al. Frequent incidental discovery of phaeochromocytoma: Data from a German cohort of 201 phaeochromocytoma. Eur J Endocrinol. 2009;161(2):355–61. http://dx.doi.org/10.1530/EJE-09-0384
4. Farrugia FA, Martikos G, Tzanetis P, Charalampopoulos A, Misiakos E, Zavras N, et al. Pheochromocytoma, diagnosis and treatment: Review of the literature. Endocr Regul. 2017;51(3):168–81. http://dx.doi.org/10.1515/enr-2017-0018
5. Fishbein L, Merrill S, Fraker DL, Cohen DL, Nathanson KL. Inherited mutations in pheochromocytoma and paraganglioma: Why all patients should be offered genetic testing. Ann Surg Oncol. 2013;20(5):1444–50. http://dx.doi.org/10.1245/s10434-013-2942-5
6. Ctvrtlik F, Koranda P, Schovanek J, Skarda J, Hartmann I, Tudos Z. Current diagnostic imaging of pheochromocytomas and implications for therapeutic strategy. Exp Ther Med. 2018;15(4):3151–60. http://dx.doi.org/10.3892/etm.2018.5871
7. Baez JC, Jagannathan JP, Krajewski K, O'Regan K, Zukotynski K, Kulke M, et al. Pheochromocytoma and paraganglioma: Imaging characteristics. Cancer Imaging. 2012;12:153–62. http://dx.doi.org/10.1102/1470-5206.2012.0016
8. Favier J, Briere JJ, Strompf L, Amar L, Filali M, Jeunemaitre X, et al. Hereditary paraganglioma/pheochromocytoma and inherited succinate dehydrogenase deficiency. Horm Res. 2005;63(4):171–9. http://dx.doi.org/10.1159/000084685
9. Grogan RH, Mitmaker EJ, Duh QY. Changing paradigms in the treatment of malignant pheochromocytoma. Cancer Control. 2011;18(2):104–12. http://dx.doi.org/10.1177/107327481101800205
10. Leung K, Stamm M, Raja A, Low G. Pheochromocytoma: The range of appearances on ultrasound, CT, MRI, and functional imaging. AJR Am J Roentgenol. 2013;200(2):370–8. http://dx.doi.org/10.2214/AJR.12.9126
11. Brown ML, Zayas GE, Abel MD, Young WF Jr, Schaff HV. Mediastinal paragangliomas: The mayo clinic experience. Ann Thorac Surg. 2008;86(3):946–51. http://dx.doi.org/10.1016/j.athoracsur.2008.04.105

12. Wen J, Li HZ, Ji ZG, Mao QZ, Shi BB, Yan WG. A decade of clinical experience with extra-adrenal paragangliomas of retroperitoneum: Report of 67 cases and a literature review. Urol Ann. 2010;2(1):12–16. http://dx.doi.org/10.4103/0974-7796.62919
13. Ayala-Ramirez M, Feng L, Johnson MM, Ejaz S, Habra MA, Rich T, et al. Clinical risk factors for malignancy and overall survival in patients with pheochromocytomas and sympathetic paragangliomas: Primary tumor size and primary tumor location as prognostic indicators. J Clin Endocrinol Metab. 2011;96(3):717–25. http://dx.doi.org/10.1210/jc.2010-1946
14. Disick GI, Palese MA. Extra-adrenal pheochromocytoma: Diagnosis and management. Curr Urol Rep. 2007;8(1):83–8. http://dx.doi.org/10.1007/s11934-007-0025-5
15. Tsirlin A, Oo Y, Sharma R, Kansara A, Gliwa A, Banerji MA. Pheochromocytoma: A review. Maturitas. 2014;77(3):229–38. http://dx.doi.org/10.1016/j.maturitas.2013.12.009
16. Hamrahian AH, Ioachimescu AG, Remer EM, Motta-Ramirez G, Bogabathina H, Levin HS, et al. Clinical utility of noncontrast computed tomography attenuation value (hounsfield units) to differentiate adrenal adenomas/hyperplasias from nonadenomas: Cleveland Clinic experience. J Clin Endocrinol Metab. 2005;90(2):871–7. http://dx.doi.org/10.1210/jc.2004-1627
17. Motta-Ramirez GA, Remer EM, Herts BR, Gill IS, Hamrahian AH. Comparison of CT findings in symptomatic and incidentally discovered pheochromocytomas. AJR Am J Roentgenol. 2005;185(3):684–8. http://dx.doi.org/10.2214/ajr.185.3.01850684
18. Park BK, Kim CK, Kwon GY, Kim JH. Re-evaluation of pheochromocytomas on delayed contrast-enhanced CT: Washout enhancement and other imaging features. Eur Radiol. 2007;17(11):2804–9. http://dx.doi.org/10.1007/s00330-007-0695-x
19. Lee KY, Oh YW, Noh HJ, Lee YJ, Yong HS, Kang EY, et al. Extraadrenal paragangliomas of the body: Imaging features. AJR Am J Roentgenol. 2006;187(2):492–504. http://dx.doi.org/10.2214/AJR.05.0370
20. Woo S, Suh CH, Kim SY, Cho JY, Kim SH. Pheochromocytoma as a frequent false-positive in adrenal washout CT: A systematic review and meta-analysis. Eur Radiol. 2018;28(3):1027–36. http://dx.doi.org/10.1007/s00330-017-5076-5
21. Patel J, Davenport MS, Cohan RH, Caoili EM. Can established CT attenuation and washout criteria for adrenal adenoma accurately exclude pheochromocytoma? AJR Am J Roentgenol. 2013;201(1):122–7. http://dx.doi.org/10.2214/AJR.12.9620
22. Baid SK, Lai EW, Wesley RA, Ling A, Timmers HJ, Adams KT, et al. Brief communication: Radiographic contrast infusion and catecholamine release in patients with pheochromocytoma. Ann Intern Med. 2009;150(1):27–32. http://dx.doi.org/10.7326/0003-4819-150-1-200901060-00006
23. Varghese JC, Hahn PF, Papanicolaou N, Mayo-Smith WW, Gaa JA, Lee MJ. MR differentiation of phaeochromocytoma from other adrenal lesions based on qualitative analysis of T2 relaxation times. Clin Radiol. 1997;52(8):603–6. http://dx.doi.org/10.1016/S0009-9260(97)80252-8
24. Adam SZ, Nikolaidis P, Horowitz JM, Gabriel H, Hammond NA, Patel T, et al. Chemical shift MR imaging of the adrenal gland: Principles, pitfalls, and applications. Radiographics. 2016;36(2):414–32. http://dx.doi.org/10.1148/rg.2016150139
25. Blake MA, Kalra MK, Maher MM, Sahani DV, Sweeney AT, Mueller PR, et al. Pheochromocytoma: An imaging chameleon. Radiographics. 2004;24(Suppl 1):S87–99. http://dx.doi.org/10.1148/rg.24si045506
26. Havekes B, Lai EW, Corssmit EP, Romijn JA, Timmers HJ, Pacak K. Detection and treatment of pheochromocytomas and paragangliomas: Current standing of MIBG scintigraphy and future role of PET imaging. Q J Nucl Med Mol Imaging. 2008;52(4):419–29.
27. Beierwaltes WH. Endocrine imaging: Parathyroid, adrenal cortex and medulla, and other endocrine tumors. Part II. J Nucl Med. 1991;32(8):1627–39.
28. Ilias I, Pacak K. Current approaches and recommended algorithm for the diagnostic localization of pheochromocytoma. J Clin Endocrinol Metab. 2004;89(2):479–91. http://dx.doi.org/10.1210/jc.2003-031091
29. Bombardieri E, Giammarile F, Aktolun C, Baum RP, Bischof Delaloye A, Maffioli L, et al. 131I/123I-metaiodobenzylguanidine (mIBG) scintigraphy: Procedure guidelines for tumour imaging. Eur J Nucl Med Mol Imaging. 2010;37(12):2436–46. http://dx.doi.org/10.1007/s00259-010-1545-7

30. Lumachi F, Tregnaghi A, Zucchetta P, Cristina Marzola M, Cecchin D, Grassetto G, et al. Sensitivity and positive predictive value of CT, MRI and 123I-MIBG scintigraphy in localizing pheochromocytomas: A prospective study. Nucl Med Commun. 2006;27(7):583–7. http://dx.doi.org/10.1097/00006231-200607000-00006
31. Nakatani T, Hayama T, Uchida J, Nakamura K, Takemoto Y, Sugimura K. Diagnostic localization of extra-adrenal pheochromocytoma: Comparison of (123)I-MIBG imaging and (131)I-MIBG imaging. Oncol Rep. 2002;9(6):1225–7. http://dx.doi.org/10.3892/or.9.6.1225
32. Neumann HP, Berger DP, Sigmund G, Blum U, Schmidt D, Parmer RJ, et al. Pheochromocytomas, multiple endocrine neoplasia type 2, and von Hippel-Lindau disease. N Engl J Med. 1993;329(21):1531–8. http://dx.doi.org/10.1056/NEJM199311183292103
33. Derlin T, Busch JD, Wisotzki C, Schoennagel BP, Bannas P, Papp L, et al. Intraindividual comparison of 123I-mIBG SPECT/MRI, 123I-mIBG SPECT/CT, and MRI for the detection of adrenal pheochromocytoma in patients with elevated urine or plasma catecholamines. Clin Nucl Med. 2013;38(1):e1–6. http://dx.doi.org/10.1097/RLU.0b013e318263923d
34. Milardovic R, Corssmit EP, Stokkel M. Value of 123I-MIBG scintigraphy in paraganglioma. Neuroendocrinology. 2010;91(1):94–100. http://dx.doi.org/10.1159/000242499
35. Koopmans KP, Jager PL, Kema IP, Kerstens MN, Albers F, Dullaart RP. 111In-octreotide is superior to 123I-metaiodobenzylguanidine for scintigraphic detection of head and neck paragangliomas. J Nucl Med. 2008;49(8):1232–7. http://dx.doi.org/10.2967/jnumed.107.047738
36. Nguyen HH, Proye CA, Carnaille B, Combemale F, Pattou FN, Huglo D. Tumour size: The only predictive factor for 131I MIBG uptake in phaeochromocytoma and paraganglioma. Aust N Z J Surg. 1999;69(5):350–3. http://dx.doi.org/10.1046/j.1440-1622.1999.01570.x
37. Bhatia KS, Ismail MM, Sahdev A, Rockall AG, Hogarth K, Canizales A, et al. 123I-metaiodobenzylguanidine (MIBG) scintigraphy for the detection of adrenal and extra-adrenal phaeochromocytomas: CT and MRI correlation. Clin Endocrinol (Oxf). 2008;69(2):181–8. http://dx.doi.org/10.1111/j.1365-2265.2008.03256.x
38. Tan TH, Hussein Z, Saad FF, Shuaib IL. Diagnostic performance of (68)Ga-DOTATATE PET/CT, (18)F-FDG PET/CT and (131)I-MIBG scintigraphy in mapping metastatic pheochromocytoma and paraganglioma. Nucl Med Mol Imaging. 2015;49(2):143–51. http://dx.doi.org/10.1007/s13139-015-0331-7
39. Quint LE, Glazer GM, Francis IR, Shapiro B, Chenevert TL. Pheochromocytoma and paraganglioma: Comparison of MR imaging with CT and I-131 MIBG scintigraphy. Radiology. 1987;165(1):89–93. http://dx.doi.org/10.1148/radiology.165.1.3628794
40. Shapiro B, Copp JE, Sisson JC, Eyre PL, Wallis J, Beierwaltes WH. Iodine-131 metaiodobenzylguanidine for the locating of suspected pheochromocytoma: Experience in 400 cases. J Nucl Med. 1985;26(6):576–85.
41. Meyer-Rochow GY, Schembri GP, Benn DE, Sywak MS, Delbridge LW, Robinson BG, et al. The utility of metaiodobenzylguanidine single photon emission computed tomography/computed tomography (MIBG SPECT/CT) for the diagnosis of pheochromocytoma. Ann Surg Oncol. 2010;17(2):392–400. http://dx.doi.org/10.1245/s10434-009-0850-5
42. Rozovsky K, Koplewitz BZ, Krausz Y, Revel-Vilk S, Weintraub M, Chisin R, et al. Added value of SPECT/CT for correlation of MIBG scintigraphy and diagnostic CT in neuroblastoma and pheochromocytoma. AJR Am J Roentgenol. 2008;190(4):1085–90. http://dx.doi.org/10.2214/AJR.07.2107
43. Solanki KK, Bomanji J, Moyes J, Mather SJ, Trainer PJ, Britton KE. A pharmacological guide to medicines which interfere with the biodistribution of radiolabelled meta-iodobenzylguanidine (MIBG). Nucl Med Commun. 1992;13(7):513–21. http://dx.doi.org/10.1097/00006231-199207000-00006
44. Reubi JC, Schar JC, Waser B, Wenger S, Heppeler A, Schmitt JS, et al. Affinity profiles for human somatostatin receptor subtypes SST1-SST5 of somatostatin radiotracers selected for scintigraphic and radiotherapeutic use. Eur J Nucl Med. 2000;27(3):273–82. http://dx.doi.org/10.1007/s002590050034
45. Cescato R, Schulz S, Waser B, Eltschinger V, Rivier JE, Wester HJ, et al. Internalization of sst2, sst3, and sst5 receptors: Effects of somatostatin agonists and antagonists. J Nucl Med. 2006;47(3):502–11.
46. Papotti M, Bongiovanni M, Volante M, Allia E, Landolfi S, Helboe L, et al. Expression of somatostatin receptor types 1-5 in 81 cases of gastrointestinal and pancreatic endocrine tumors. A correlative

immunohistochemical and reverse-transcriptase polymerase chain reaction analysis. Virchows Arch. 2002;440(5):461–75. http://dx.doi.org/10.1007/s00428-002-0609-x
47. Kwekkeboom DJ, Krenning EP. Somatostatin receptor imaging. Semin Nucl Med. 2002;32(2):84–91. http://dx.doi.org/10.1053/snuc.2002.31022
48. Gibril F, Reynolds JC, Chen CC, Yu F, Goebel SU, Serrano J, et al. Specificity of somatostatin receptor scintigraphy: A prospective study and effects of false-positive localizations on management in patients with gastrinomas. J Nucl Med. 1999;40(4):539–53.
49. Kwekkeboom DJ, Kam BL, van Essen M, Teunissen JJ, van Eijck CH, Valkema R, et al. Somatostatin-receptor-based imaging and therapy of gastroenteropancreatic neuroendocrine tumors. Endocr Relat Cancer. 2010;17(1):R53–73. http://dx.doi.org/10.1677/ERC-09-0078
50. van der Harst E, de Herder WW, Bruining HA, Bonjer HJ, de Krijger RR, Lamberts SW, et al. [(123)I]metaiodobenzylguanidine and [(111)In]octreotide uptake in begnign and malignant pheochromocytomas. J Clin Endocrinol Metab. 2001;86(2):685–93. https://doi.org/10.1210/jcem.86.2.7238
51. Hoefnagel CA. MIBG and radiolabeled octreotide in neuroendocrine tumors. Q J Nucl Med. 1995;39(4 Suppl 1):137–9.
52. Buchmann I, Henze M, Engelbrecht S, Eisenhut M, Runz A, Schafer M, et al. Comparison of 68Ga-DOTATOC PET and 111In-DTPAOC (Octreoscan) SPECT in patients with neuroendocrine tumours. Eur J Nucl Med Mol Imaging. 2007;34(10):1617–26. http://dx.doi.org/10.1007/s00259-007-0450-1
53. Taieb D, Sebag F, Barlier A, Tessonnier L, Palazzo FF, Morange I, et al. 18F-FDG avidity of pheochromocytomas and paragangliomas: A new molecular imaging signature? J Nucl Med. 2009;50(5):711–17. http://dx.doi.org/10.2967/jnumed.108.060731
54. Werner RA, Solnes LB, Javadi MS, Weich A, Gorin MA, Pienta KJ, et al. SSTR-RADS version 1.0 as a reporting system for SSTR PET imaging and selection of potential PRRT candidates: A proposed standardization framework. J Nucl Med. 2018;59(7):1085–91. http://dx.doi.org/10.2967/jnumed.117.206631
55. Boy C, Heusner TA, Poeppel TD, Redmann-Bischofs A, Unger N, Jentzen W, et al. 68Ga-DOTATOC PET/CT and somatostatin receptor (sst1-sst5) expression in normal human tissue: Correlation of sst2 mRNA and SUVmax. Eur J Nucl Med Mol Imaging. 2011;38(7):1224–36. http://dx.doi.org/10.1007/s00259-011-1760-x
56. Wild D, Schmitt JS, Ginj M, Macke HR, Bernard BF, Krenning E, et al. DOTA-NOC, a high-affinity ligand of somatostatin receptor subtypes 2, 3 and 5 for labelling with various radiometals. Eur J Nucl Med Mol Imaging. 2003;30(10):1338–47. http://dx.doi.org/10.1007/s00259-003-1255-5
57. Bozkurt MF, Virgolini I, Balogova S, Beheshti M, Rubello D, Decristoforo C, et al. Guideline for PET/CT imaging of neuroendocrine neoplasms with (68)Ga-DOTA-conjugated somatostatin receptor targeting peptides and (18)F-DOPA. Eur J Nucl Med Mol Imaging. 2017;44(9):1588–601. http://dx.doi.org/10.1007/s00259-017-3728-y
58. Cherk MH, Kong G, Hicks RJ, Hofman MS. Changes in biodistribution on (68)Ga-DOTA-Octreotate PET/CT after long acting somatostatin analogue therapy in neuroendocrine tumour patients may result in pseudoprogression. Cancer Imaging. 2018;18(1):3. http://dx.doi.org/10.1186/s40644-018-0136-x
59. Moreau A, Giraudet AL, Kryza D, Borson-Chazot F, Bournaud-Salinas C, Mognetti T, et al. FDOPA patterns in adrenal glands: A pictorial essay. Clin Nucl Med. 2017;42(5):379–82. http://dx.doi.org/10.1097/RLU.0000000000001636
60. Pandit-Taskar N, Zanzonico P, Staton KD, Carrasquillo JA, Reidy-Lagunes D, Lyashchenko S, et al. Biodistribution and dosimetry of (18)F-meta-fluorobenzylguanidine: A first-in-human PET/CT imaging study of patients with neuroendocrine malignancies. J Nucl Med. 2018;59(1):147–53. http://dx.doi.org/10.2967/jnumed.117.193169
61. Gonias S, Goldsby R, Matthay KK, Hawkins R, Price D, Huberty J, et al. Phase II study of high-dose [131I]metaiodobenzylguanidine therapy for patients with metastatic pheochromocytoma and paraganglioma. J Clin Oncol. 2009;27(25):4162–8. http://dx.doi.org/10.1200/JCO.2008.21.3496

62. Loh KC, Fitzgerald PA, Matthay KK, Yeo PP, Price DC. The treatment of malignant pheochromocytoma with iodine-131 metaiodobenzylguanidine (131I-MIBG): A comprehensive review of 116 reported patients. J Endocrinol Invest. 1997;20(11):648–58. http://dx.doi.org/10.1007/BF03348026
63. Baum RP, Kulkarni HR, Carreras C. Peptides and receptors in image-guided therapy: Theranostics for neuroendocrine neoplasms. Semin Nucl Med. 2012;42(3):190–207. http://dx.doi.org/10.1053/j.semnuclmed.2012.01.002
64. Bodei L, Mueller-Brand J, Baum RP, Pavel ME, Horsch D, O'Dorisio MS, et al. The joint IAEA, EANM, and SNMMI practical guidance on peptide receptor radionuclide therapy (PRRNT) in neuroendocrine tumours. Eur J Nucl Med Mol Imaging. 2013;40(5):800–16. http://dx.doi.org/10.1007/s00259-012-2330-6
65. Kwekkeboom DJ, de Herder WW, Kam BL, van Eijck CH, van Essen M, Kooij PP, et al. Treatment with the radiolabeled somatostatin analog [177 Lu-DOTA 0,Tyr3]octreotate: Toxicity, efficacy, and survival. J Clin Oncol. 2008;26(13):2124–30. http://dx.doi.org/10.1200/JCO.2007.15.2553
66. Paganelli G, Sansovini M, Ambrosetti A, Severi S, Monti M, Scarpi E, et al. 177 Lu-Dota-octreotate radionuclide therapy of advanced gastrointestinal neuroendocrine tumors: Results from a phase II study. Eur J Nucl Med Mol Imaging. 2014;41(10):1845–51. http://dx.doi.org/10.1007/s00259-014-2735-5
67. Strosberg J, El-Haddad G, Wolin E, Hendifar A, Yao J, Chasen B, et al. Phase 3 trial of (177)Lu-dotatate for midgut neuroendocrine tumors. N Engl J Med. 2017;376(2):125–35. http://dx.doi.org/10.1056/NEJMoa1607427
68. van Vliet EI, Krenning EP, Teunissen JJ, Bergsma H, Kam BL, Kwekkeboom DJ. Comparison of response evaluation in patients with gastroenteropancreatic and thoracic neuroendocrine tumors after treatment with [177Lu-DOTA0,Tyr3]octreotate. J Nucl Med. 2013;54(10):1689–96. http://dx.doi.org/10.2967/jnumed.112.117408